

The spin-dependence of the Blandford-Znajek effect

David Garofalo¹

ABSTRACT

The interaction of large scale magnetic fields with the event horizon of rotating black holes (the Blandford-Znajek [1977] mechanism) forms the basis for some models of the most relativistic jets. We explore a scenario in which the central inward “plunging” region of the accretion flow enhances the trapping of large scale poloidal field on the black hole. The study is carried out using a fully relativistic treatment in Kerr spacetime, with the focus being to determine the spin dependence of the Blandford-Znajek effect. We find that large scale magnetic fields are enhanced on the black hole compared to the inner accretion flow and that the ease with which this occurs for lower prograde black hole spin, produces a spin dependence in the Blandford-Znajek effect that has attractive applications to recent observations. Among these is the correlation between inferred accretion rate and nuclear jet power observed by Allen et al. (2006) in X-ray luminous elliptical galaxies. If the black hole rotation in these elliptical galaxies is in the prograde sense compared with that of the inner accretion disk, we show that both the absolute value and the uniformity of the implied jet-production efficiency can be explained by the flux-trapping model. The basic scenario that emerges from this study is that a range of intermediate values of black hole spins could be powering these AGN. We also suggest that the jets in the most energetic radio-galaxies may be powered by accretion onto *retrograde* rapidly-rotating black holes.

1. Introduction

Astrophysical jets appear to be ubiquitous in accreting systems surrounded by magnetic fields. Although the precise mechanism by which magnetic fields aid in the production of jets is unknown, there are two basic models that may account for the phenomenon. The first involves a magnetocentrifugal or magnetohydrodynamic (MHD) wind (Blandford & Payne 1982). Closely related to the solar wind phenomenon, an accretion disk threaded by large scale magnetic field extracts plasma

¹Jet Propulsion Laboratory, California Institute of Technology, Pasadena CA 91109. email: David.A.Garofalo@jpl.nasa.gov

from the disk and expels it along the fieldlines that extend far away from the source. Evidence for uncollimated MHD winds has recently been found in Galactic Black Hole Binaries (GBHBs) by Miller et al (2006), and such winds may be responsible for the warm absorber in many active galactic nuclei (AGN; Reynolds 1997; McKernan et al. 2007). Despite possessing the appealing feature of being applicable to outflows from all accreting sources from compact stars like white dwarfs and neutron stars up to surfaceless objects such as black holes as well as forming stars, the MHD wind model may fail to explain the highly relativistic, possibly pair-dominated (Reynolds et al. 1996; Wardle et al. 1998) jets observed from some AGN. The second class of models applies only to black hole accretors, invoking a direct connection between the magnetic field and the rotating spacetime of spinning black holes which allows for black hole spin-energy extraction (Blandford & Znajek, 1977, henceforth BZ). In the BZ mechanism, the power extracted is related to the dimensionless spin parameter a and the horizon-threading magnetic field B_H via

$$L_{BZ} \approx \frac{1}{32} \frac{\Omega_F(\Omega_H - \Omega_F)}{\Omega_H^2} B_H^2 r_H^2 a^2 c \quad (1)$$

where Ω_F is the angular velocity of observers that measure zero electric field, Ω_H is the angular velocity of the black hole event horizon, r_H is the radius of the event horizon in Boyer-Lindquist coordinates, and B_H is the normal hole-threading magnetic field, which means that larger hole-threading fields lead to greater BZ luminosity. Although this dependence was originally obtained in the low spin limit, Komissarov (2001) has performed a numerical study of the BZ solution concluding that the dependence on spin in equation 1 is valid at least up to $a = 0.9$. For completeness, a model that also involves black hole rotational energy extraction via plasma on negative energy orbits in the ergosphere was developed by Punsly & Coroniti (1991); and, a model that involves a combination of the BZ and BP effects was developed by Meier (1999).

Until the early 1990's, the maximum strength of the hole-threading magnetic field was determined by considering the strength of the disk-threading field. If the horizon-threading field exceeded the large scale field of the accretion disk, the argument went, the former would push its way off the hole via magnetic pressure, back into the disk until the hole-threading field strength was comparable to the disk field strength. Two major untested assumptions go into this scenario. The first is that the hole-threading field is confined via Maxwell pressure by the disk-threading field, while the second is that the disk-threading field grows to a large enough value to confine a black hole threading field sufficient to drive a powerful jet via the BZ process.

In seminal work, Balbus & Hawley (1991) realized that astrophysical accretion disks are subject to a powerful MHD instability (previously discussed by Chandrasekhar [1960] and Velikhov [1959]), and that the resulting MHD turbulence is likely to be responsible for the angular momentum transport that facilitates accretion. However, a consequence of this realization is that the disk magnetic field must be characteristically weak (in the sense that gas pressure must exceed magnetic pressure by an order of magnitude or else the MRI is suppressed). This forms the basis for

the arguments of Lubow (1994), Ghosh & Abramowicz (1997), and Livio et al (1999), pointing to basic constraints on the strength of the hole-threading field. Essentially, these authors argue that if the magnetic field threading the black hole greatly exceeds the large scale field threading the disk, the hole-threading field expands back into the accretion disk until an approximate balance is achieved. If this were the case, the resulting weak field threading the black hole would be insufficient to explain the most powerful AGN jets we see.

In Reynolds, Garofalo & Begelman (2006; hereafter RGB) we challenged the argument that Maxwell pressure from the disk solely determines the field on the hole on the basis that such a conclusion ignores the dynamics of the accretion flow within the radius of marginal stability. Within this radius, circular orbits are no longer stable and the accretion flow plunges into the black hole. Hereafter we refer to the region within the radius of marginal stability as the “plunge region”. In RGB, we argue that the inertial forces within the plunge region prevent magnetic field that is threading the black hole from expanding back into the disk. Accretion of magnetic field can result in a strong flux-bundle threading the black hole, confined in the disk plane by the plunge region. This flux bundle does, however, expand at high latitudes due to Maxwell pressure. Steady-state is obtained when field lines threading the inner disk are bent by the high latitude regions of the flux bundle such that tension-induced outwards diffusion of the field line through the accretion disk balances inwards advection of the field line.

In this paper, we adopt the formalism of RGB and extend it to the relativistic regime in order to determine the spin dependence of magnetic flux accumulation on the black hole. We also show that the $a = 0$ limit produces flux accumulation values close to those obtained in the non-relativistic study, establishing the validity of the RGB results for slowly spinning black holes. Our central result is that the ability of the plunge region to enhance the black hole threading field decreases as the spin of the black hole increases. Despite this decrease in the ability of the plunge region to produce a black hole-threading field that is enhanced with respect to the inner accretion flow, the hole-threading field is always greater than the field strength in the inner accretion flow. This means that the BZ power in our model is always greater than in “classical” BZ where this enhancement is not included. In Section 2, we describe the formalism of the relativistic extension of the flux-trapping model. We discuss the covariant nature of the magnetic flux function and the equations it satisfies. In Section 3 we present our results and show that the hole-threading flux decreases with increase in spin for lower prograde spins. This appears to be largely a geometrical effect connected to the radial position of the marginally stable orbit and the horizon as a function of spin. In section 4, we discuss the implications of our model in view of the recently discovered correlation between jet power and accretion rate found by Allen et al. (2006). Our model also predicts that accretion onto rapidly rotating *retrograde* black holes will produce extremely powerful jets, and we suggest this as a mechanism for powering the most luminous radio-loud AGN. Section 6 presents our conclusions.

2. Relativistic Generalization of the Flux-Trapping Model

Our goal is to construct a relativistic version of the model described by RGB. We consider a geometrically-thin accretion disk around a Kerr black hole threaded by a large scale magnetic field. On small scales, the magnetic field lines are frozen into the highly conductive plasma of the accretion disk. However, if we coarse-grain our view to larger scales, we expect that the large scale magnetic field lines can undergo turbulent diffusion through the disk plasma. Heyvaerts et al. (1996) have shown that the effective magnetic Prandtl number (i.e., the ratio of the effective turbulent viscosity to the effective turbulent magnetic diffusivity) is expected to be within an order of magnitude of unity. Hence a field line threading the disk will be dragged inwards by accretion, but radial magnetic pressure gradients and magnetic tension (associated with field line curvature as it threads the disk) will lead to competitive field line diffusion. We assume the region above and below the disk has a very low plasma density, and hence for the magnetic field in this region to have a force-free configuration. As argued by RGB, field lines threading through the plunge region of the accretion flow will be dragged very rapidly onto the black hole, leaving the plunge region devoid of poloidal magnetic flux.

Below we describe the idealizations and construction of our model system.

1. Our accretion disk is described by a Novikov & Thorne (1974) disk truncated at the marginally stable orbit, inwards of which is the plunging region. We assume that the large scale magnetic field does not perturb the structure of the turbulent accretion flow.
2. In the magnetosphere (the region outside of the black hole and accretion disk) we assume that the plasma density is negligible and hence that the magnetic field is force free and we impose a current density distribution that is compatible with the horizon regularity condition (see below).
3. As discussed above, we assume that no poloidal magnetic flux threads the plunge region of the accretion disk. Any magnetic flux that is advected inwards across the radius of marginal stability is immediately added to the flux bundle threading the black hole. This is the distinguishing fundamental assumption of our model.
4. The boundary condition on the horizon requires imposing finite electric and magnetic fields as measured by freely-falling observers crossing the horizon. Znajek (1978) worked out the appropriate boundary, or regularity, condition on the horizon under this assumption for a force-free magnetosphere. This condition is imposed on the horizon in our model.
5. Far away from the black hole and at poloidal angles above the accretion disk, we assume the large-scale field is uniform and impose an appropriate outer boundary condition that

captures this assumption. Far away from the black hole but in the plane of the accretion disk we impose a “dead zone” as in RGB. The only difference between this region and the active disk region is that the radial inflow velocity is set to zero. In the dead zone, therefore, magnetic field lines are not dragged toward the black hole. As pointed out in greater detail in RGB, this dead zone dramatically reduces the sensitivity of the system to the treatment of the outer boundary. The physical nature of the dead zone which is addressed in RGB, allows us to smoothly truncate the accretion disk. The outer boundary condition applied here amounts to bounding the system with a perfectly conducting sphere. This differs from RGB who, due to the analytic techniques possible in the non-relativistic problem, could bound the system in the plane by a large conducting annulus, and otherwise just apply boundary conditions at infinity out of the plane.

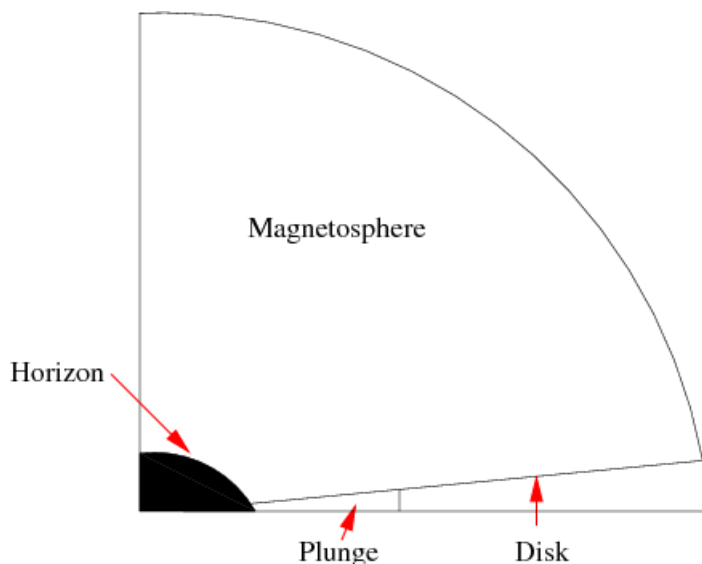


Fig. 1.—: Boundaries for the axisymmetric numerical solutions

2.1. Basic equations of our model

We assume that the underlying spacetime is that of an isolated rotating black hole, i.e., that the gravitational field of the rotating black hole completely dominates over that of the accretion disk. Throughout this paper, we will work in Boyer-Lindquist coordinates in which the Kerr metric

takes the standard form,

$$dS^2 = - \left(1 - \frac{2Mr}{\rho^2}\right) dt^2 - \frac{4Mar \sin^2 \theta}{\rho^2} dt d\phi \quad (2)$$

$$+ \frac{\Sigma}{\rho^2} \sin^2 \theta d\phi^2 + \frac{\rho^2}{\Delta} dr^2 + \rho^2 d\theta^2,$$

where

$$\rho^2 = r^2 + a^2 \cos^2 \theta, \quad (3)$$

$$\Delta = r^2 - 2Mr + a^2, \quad (4)$$

and

$$\Sigma = (r^2 + a^2)^2 - a^2 \Delta \sin^2 \theta. \quad (5)$$

The basic equation describing the evolution of the (large-scale) magnetic field within the accretion disk is obtained by following the relativistic analogue of the non-relativistic treatment of RGB. One difference between our approach and that of RGB is that we only seek the stationary (time-independent) solution; this results in a significant simplification in the relativistic equations that we must deal with. The equation describing the field evolution within the disk is obtained by combining Maxwell's equation

$$\nabla_b F^{ab} = \mu J^a, \quad (6)$$

with a simplified Ohm's law

$$J^a = \sigma F^{ab} u_b - u^a J_b u^b, \quad (7)$$

where F^{ab} is the standard Faraday tensor, μ is the permeability of the plasma, J^a the 4-current, u^a the 4-velocity of the accretion disk flow, and σ the effective conductivity of the turbulent plasma. This gives

$$\nabla_b F^{ab} = \frac{1}{\eta} F^{ab} u_b - \mu u^a u_b J^b, \quad (8)$$

where $\eta = 1/\mu\sigma$ is the effective magnetic diffusivity. To reiterate, the microscopic magnetic diffusivity of the plasma is expected to be essentially zero. However, in a coarse-grained view, magnetic field lines will diffuse through the turbulent plasma due to small scale reconnection events, and it is this process that is parametrized through the effective magnetic diffusivity. The second term on the right-hand side of equation 8, which we include for completeness, is zero by the MHD assumption that proper electric charge vanishes. Therefore, the disk is governed by

$$\nabla_b F^{ab} = \frac{1}{\eta} F^{ab} u_b. \quad (9)$$

The equations are cast in terms of the vector potential, which is related to the Faraday tensor via

$$F_{ab} = A_{b,a} - A_{a,b}, \quad (10)$$

and, in particular, in terms of the component A_ϕ in the coordinate basis of the Boyer-Lindquist coordinates.

Ultimately, to examine BZ powers, we need to derive the magnetic flux threading a hoop placed at a given radius r . The magnetic flux function is related to the vector potential via Stokes' Theorem applied to the Faraday tensor

$$\psi \equiv \int_S F = \int_S dA = \int_{\partial S} A = 2\pi A_\phi, \quad (11)$$

where S is a space-like surface with boundary ∂S consisting of a ring defined by $r = \text{constant}$, $\theta = \text{constant}$, and $t = \text{constant}$. Because we work with the vector potential, A_b , we comment briefly on the choice of gauge. Since A_b is specified up to the gradient of a scalar function Γ ,

$$A'_b = A_b + \nabla_b \Gamma, \quad (12)$$

the assumption of time-independence and axisymmetry gives us

$$A'_t = A_t \quad (13)$$

and

$$A'_\phi = A_\phi. \quad (14)$$

Thus, we need not specify the gauge uniquely beyond the statement of t and ϕ independence. Writing the ϕ component of eqn. 9 in terms of the vector potential, and applying time-independence and axisymmetry yields,

$$\begin{aligned} & \frac{\partial}{\partial r} \left[g^{11} \left(g^{30} \frac{\partial A_t}{\partial r} + g^{33} \frac{\partial A_\phi}{\partial r} \right) \right] + \frac{\partial}{\partial \theta} \left[g^{22} \left(g^{30} \frac{\partial A_t}{\partial \theta} + g^{33} \frac{\partial A_\phi}{\partial \theta} \right) \right] + \quad (15) \\ & \frac{1}{2} \left(g^{00} \frac{\partial g_{00}}{\partial r} + 2g^{30} \frac{\partial g_{30}}{\partial r} + g^{33} \frac{\partial g_{33}}{\partial r} + g^{11} \frac{\partial g_{11}}{\partial r} + g^{22} \frac{\partial g_{22}}{\partial r} \right) g^{11} \left(g^{30} \frac{\partial A_t}{\partial r} + g^{33} \frac{\partial A_\phi}{\partial r} \right) + \\ & \frac{1}{2} \left(g^{00} \frac{\partial g_{00}}{\partial \theta} + 2g^{30} \frac{\partial g_{30}}{\partial \theta} + g^{33} \frac{\partial g_{33}}{\partial \theta} + g^{11} \frac{\partial g_{11}}{\partial \theta} + g^{22} \frac{\partial g_{22}}{\partial \theta} \right) g^{22} \left(g^{30} \frac{\partial A_t}{\partial \theta} + g^{33} \frac{\partial A_\phi}{\partial \theta} \right) \\ & = \frac{1}{\eta} u_r g^{11} \left(g^{30} \frac{\partial A_t}{\partial r} + g^{33} \frac{\partial A_\phi}{\partial r} \right), \end{aligned}$$

where the $g_{\alpha\beta}$ and $g^{\alpha\beta}$ are the lower and upper metric terms in the Boyer-Lindquist coordinates, and are evaluated at the disk surface [$\theta = \pi/2 - \tan^{-1}(h/r)$ where h/r is the fractional thickness of the disk]. This is our final equation describing the magnetic flux threading the accretion disk.

As in the non-relativistic case (RGB), we need to match the field in the disk onto the magnetospheric field in order to fully specify the solution. As described previously, our assumptions for the magnetosphere lead to the force-free condition

$$F^{ab} J_b = 0 \quad (16)$$

and

$$\nabla_b F^{ab} = \mu J^a. \quad (17)$$

In the magnetosphere we also impose the ideal MHD condition

$$F^{ab} u_b = 0, \quad (18)$$

where u^b is the 4-velocity of the (tenuous) plasma in the magnetosphere and is determined by the condition that (in steady-state) field lines rigidly rotate.

Our basic philosophy is to solve eqn. 17 supplemented by the constraints given by equations 16 and 18 for the magnetic field structure in the magnetosphere using eqn. 15 as a boundary condition to be applied on the disk surface. Additional boundary conditions are required. The magnetic flux is fixed to be zero on the black hole spin axis (i.e., the field is assumed to be finite on the axis). We bound the region under consideration by an outer spherical boundary at large r , and assume that the flux threading that boundary corresponds to a uniform field with strength B_0 , i.e., we set $\psi = r^2 \sin^2 \theta B_0$. The regularity condition on the horizon is determined by the Znajek condition (Znajek 1978; Macdonald 1984) with explicit form,

$$\psi = \frac{2\psi_0}{1 + [\sin^2 \theta / (1 - \cos \theta)^2] \exp[-2a^2 \cos \theta / (r_+^2 + a^2)]}, \quad (19)$$

where r_+ is the radial coordinate of the horizon and ψ_0 is the magnitude of the flux threading the horizon which is determined by the numerical solution. In essence, the regularity condition imposed on the horizon amounts to the a and θ dependence of the above function only. Finally, the fundamental assumption of our model is that no poloidal magnetic flux threads the plunging region of the disk ($r_{\text{evt}} < r < r_{\text{ms}}; \theta = \pi/2 - \tan^{-1}(h/r)$). The prescription for the 4-velocity comes from the assumption that flux tubes rigidly rotate. Flux tubes that intersect the black hole all rigidly rotate but at values that depend on the polar angle whereas flux tubes that intersect the disk rotate rigidly at a Keplerian frequency determined at the disk surface except for the inner disk where the plunge region approaches. The prescription of field line rotation is such that at large polar angles, the field lines threading the horizon rotate at values that approach those of the field lines that intersect the inner accretion flow. These features exist to avoid the presence of discontinuities in the current prescription. The current prescription, on the other hand, is fixed on the polar axis and needs to be determined on the disk surface as the flux function does via a relaxation approach. In general, on the horizon and outer boundary, a regularity condition needs to be imposed (Macdonald & Thorne, 1982; Uzdensky, 2005). However, the prescription for the rigid rotation of flux tubes is chosen to avoid having to deal with an outer light cylinder, thereby allowing one to provide a simple boundary condition for the current as done for the flux function itself. This prescription simplifies calculations. On the horizon, instead, a regularity condition must be enforced which means that the prescription in the magnetosphere must be relaxed along with the regularity condition on the horizon until the two are compatible.

2.2. Solution method

We adopt a relaxation method approach to solve for the time-independent magnetic flux configuration around a Kerr black hole. Through this relaxation process, we derive the steady-state solution to equation 17 subject to constraints 16 and 18 given the boundary conditions discussed above. At the start of the numerical solution, we thread the accretion disk with uniform magnetic field everywhere which is not a steady-state solution to equation 15. We then jointly relax the magnetic configuration both in the magnetosphere and on the disk surface until a solution to equations 17 and 15 is obtained. As the solution evolves, the magnetic flux at the disk inner edge changes. As previously mentioned, a consequence of our boundary condition on the plunge region is that any magnetic flux advected across the radius of marginal stability is immediately added to the flux bundle threading the black hole. As the disk supplies flux to the horizon via the plunge region, Maxwell pressure will lead to a high-latitude expansion of the hole-threading flux bundle, changing the field geometry in the magnetosphere away from the uniform initial state. As this happens, the diffusion terms in equation 15 increase.

Flux accumulation occurs even once the hole-threading field is significantly greater than the disk-threading field because the plunge region is shielding the disk-field from the magnetic pressure associated with the hole-threading field. However, the system does settle into steady-state when the disk-threading field is bent by the expanded black hole flux-bundle such that outward field line diffusion balances inward advection. The physics is similar to that described in RGB with the exception of the presence of finite poloidal currents in the magnetosphere as well as relativistic vs. Newtonian spacetime.

In our canonical numerical solution, space is divided into a (r, θ) -grid, with 72 zones in r and 51 zones in θ . The radial coordinate runs from the horizon to an outer boundary at $r = 53$, and is spaced in a geometric progression such as to give a factor of almost 2 difference in the zone spacing at the inner and outer boundary. The θ coordinate runs from the axis ($\theta = 0$) to the disk surface, and is uniformly spaced in $\cos \theta$.

2.3. Newtonian vs. relativistic treatments of non-rotating black holes

In this section we show that the Newtonian analysis of RGB accurately describes the physics of the flux-dragging model in the slowly rotating black hole case. We choose to compare the flux-trapping that results for $a = 0$ against a Newtonian treatment, with magnetic Prandtl number fixed at $Pr_m = 20$ and varying disk thickness. Given our different treatment of the outer boundary condition, it would be inappropriate to compare our Schwarzschild results directly with the results of RGB, however. Instead, we use our code to derive both the Schwarzschild results and the

Newtonian limit ($c \rightarrow \infty$). The results are displayed in Fig. 2, where, to be consistent with the notation of RGB, we plot the ratio $\frac{A_*}{B_0}$ where $A_* = A_\phi$. The difference between the Newtonian and relativistic cases for all disk thicknesses is a few percent. This demonstrates that the neglect of the relativistic terms for slowly rotating black holes is justified, as hypothesized by RGB.

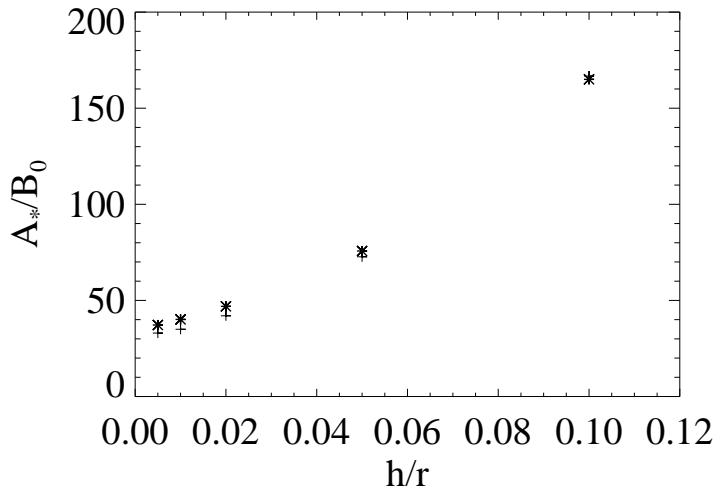


Fig. 2.—: Equilibrium value of A_*/B_0 as a function of h/r for $Pr_m=20.0$ for Newtonian (asterisk) and Schwarzschild disk (cross). Notice how the Newtonian values are larger and by a greater amount for smaller disk thickness. As the thickness increases the difference between Newtonian and Schwarzschild decreases until for largest thickness the Schwarzschild value overtakes the Newtonian. Nevertheless, the differences are always of a few percent, establishing the fact that the Newtonian treatment is sufficiently accurate for slowly rotating black holes.

2.4. Resolution and convergence study

It is necessary to confirm that our results do not rely on our particular choice of numerical resolution. We chose to examine the effects of resolution on a representative model with $a = 0.4$, $h/r = 0.1$, and $Pr_m = 20$, increasing in resolution from our canonical 72 by 51 case to 144 by 102. The results can be seen in Table 1, where we compare the equilibrium hole-threading flux of each case with that obtained at our canonical resolution. It can be seen that the higher resolution run agrees very well with a hole-threading flux that is only 1.5% lower despite quadrupling the number of computational cells. We then show the convergence to the relaxation solution. In Figure 3 we show the dependence of the flux function on the relaxation parameter t for the specific value of

$a = 0.2$. This behavior is typical for all spin runs.

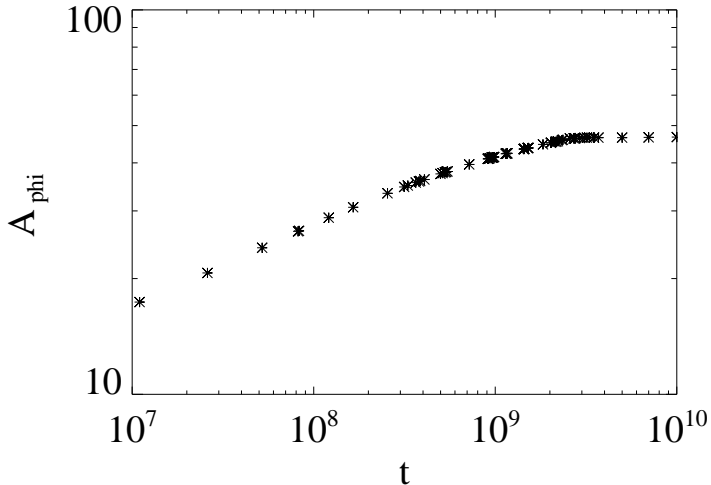


Fig. 3.—: Value of A_ϕ as a function of the relaxation parameter t showing the typical behavior of the runs. This one is for $a = 0.2$.

3. Results: spin dependence of flux trapping

We evaluate the steady-state solution to the above equations for various black hole spin values and for a range of magnetic Prandtl numbers from $Pr_m = 20$ to $Pr_m = 2$, a disk thickness of $h/r = 0.1$, $r_{dead} = 40r_g$ and $r_{out} = 53r_g$. We find that the flux accumulated on the black hole horizon decreases as the spin increases from -0.9 up to about 0.6 , beyond which the flux is roughly constant (figure 4).

The reason behind the decrease in flux with increase in spin appears to have a straightforward

spin	$r \times \theta$ grid	ψ_{norm}	% difference
0.4	72 by 51	1	0
0.4	100 by 51	1.004	0.4
0.4	100 by 80	0.985	1.5
0.4	144 by 102	1.01	1.1

Table 1:: Resolution study for flux obtained at $a = 0.4$.

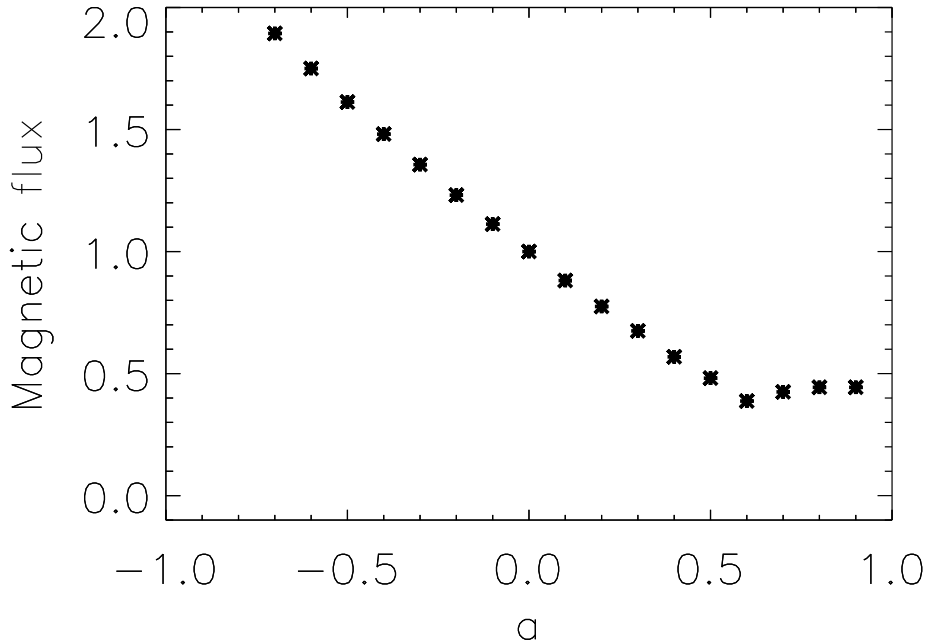


Fig. 4.—: Magnetic flux through a polar cap on the horizon normalized to the flux in the spin-zero case, vs. black hole spin illustrating the basic result that flux-trapping is less effective as the spin increases up to intermediate values of prograde spins.

geometrical interpretation. As the spin of the hole increases, the accretion disks’ inner edge (at the radius of marginal stability) gets closer to the horizon in both coordinate and proper distance. This results in a decrease of the ratio of the area within the plunge region to the area of the event horizon. Thus, as one considers more rapidly rotating black holes, the geometry becomes progressively less favorable to shielding the turbulent accretion disk from the hole-threading flux bundle. We show the geometry of magnetic flux lines for $a = 0.9$ in Fig. 5 and $a = -0.9$ in Fig. 6.

As mentioned above, the behavior of the radius of marginal stability for rapidly prograde spinning black holes results in ineffective shielding of the hole-threading flux bundle from the turbulent (diffusive) portion of the accretion disk. In short, flux-trapping breaks down for largest prograde spin, so the magnetic field threading the horizon is not enhanced and thus is equal in strength to that at the disk inner edge. Our runs, however, are done up to spin of 0.9 where the enhancement is smaller but still nonzero (i.e. the ability of the plunge region to enhance the field has not dropped to zero). Despite a decrease in size of the plunging region as spin increases, the flux values do not drop further at spins above about 0.6. Therefore, the size of the plunging region

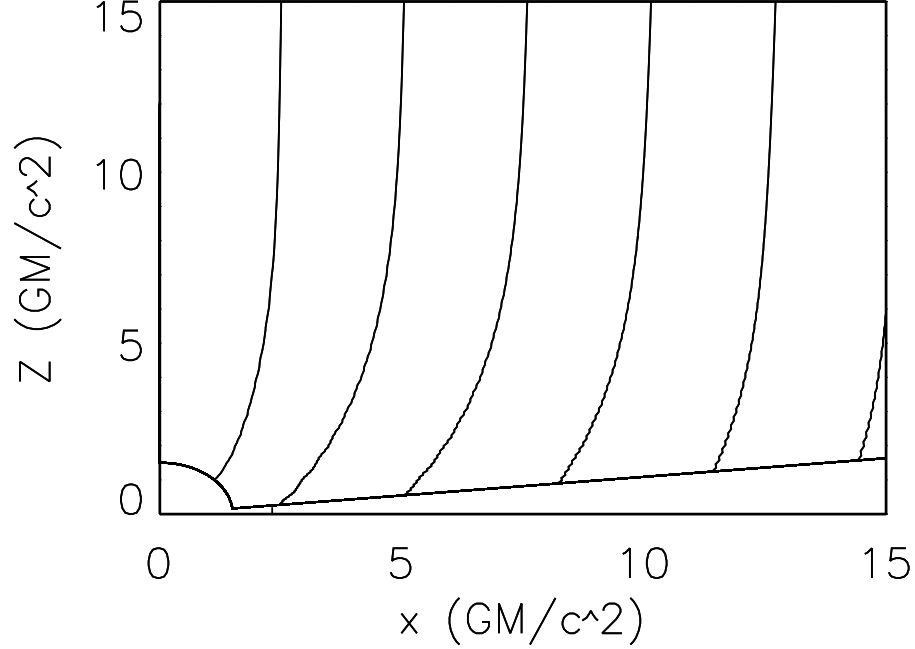


Fig. 5.—: Magnetic flux configuration for black hole with $a = 0.9$. Each side is 15 Boyer-Lindquist radii. The small vertical line at $x \approx 2.3$ indicates the marginally stable orbit, inwards of which is the plunging region

does not solely determine the dynamics of magnetic flux accumulation on the black hole; but, MHD effects at higher prograde spins kick in to attempt to increase the black hole-threading flux.

We now consider the BZ power that results from the trapped magnetic flux and its dependence on black hole spin. We start by evaluating the horizon-threading magnetic field as measured by ZAMO observers from the flux values we obtain,

$$B_H = \sqrt{g_{11}} B^r \tag{20}$$

with

$$B^r = *F^{rb} u_b, \tag{21}$$

where $*F^{ab}$ is the dual Faraday tensor and u^b is the four-velocity of the ZAMO observers evaluated in the equatorial plane on the horizon membrane (in the sense of Thorne et al, 1986). The dual tensor components involve terms with derivatives of A_ϕ with respect to θ and therefore require the use of the regularity condition on the horizon membrane (eq. 19). The results depend on the value of B_0 , the initial uniform field strength threading the horizon and are displayed in Figure 7.

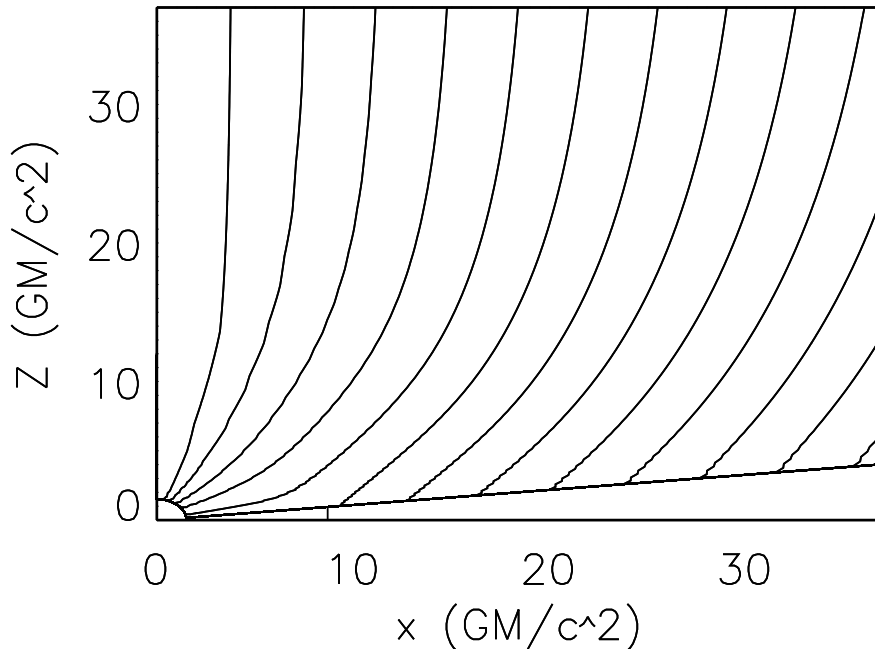


Fig. 6.—: Lines of constant magnetic flux for $a = -0.9$ retrograde spinning black hole. The axes are in BL radii. The marginally stable orbit is located at about $x = 8.7$.

With these values of the horizon-threading magnetic fields, we can determine the BZ luminosity. This is shown for prograde spins ($a > 0$) in Figure 8.

Despite possessing the largest hole-threading magnetic field for non-negative spin, the Schwarzschild case, of course, produces no BZ power. Considering prograde black holes, the maximum BZ power is generated for large a as it is for the BZ mechanism without the flux-trapping scenario. Figure 8 shows both the BZ power without flux-trapping (straight line) as well as the BZ power obtained in the flux-trapping model for a magnetic Prandtl number of 20. We note that the accumulated flux on the black hole depends linearly or almost so, on the radial coordinate value of the outer region of the active accretion disk. We have truncated the active region of our disk at $r_{dead} = 40r_g$ outwards of which the disk fluid is characterized by zero radial velocity so the dragging of flux occurs only inwards of r_{dead} . As pointed out in RGB, r_{dead} is one of the most artificial aspects of our model, but could be identified with the outer edge of the MHD-turbulence dominated accretion disk, or as the transition radius between an outer thin disk and an inner ADAF disk. We see, thus, that by increasing our active region of the disk and/or increasing the disk thickness, we could increase the generated luminosity. However, we remind the reader that our analysis is performed with large

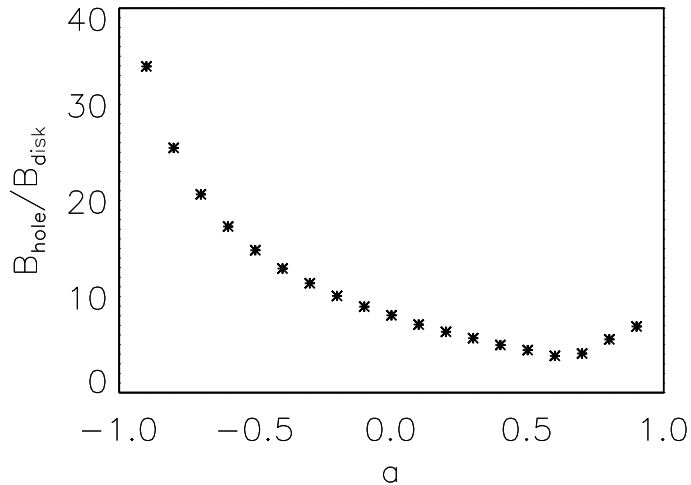


Fig. 7.—: Ratio of horizon-threading magnetic field as measured by ZAMO observers and magnetic field strength in the accretion disk as a function of spin.

magnetic Prandtl number (i.e. 20) and thus with low diffusion. RGB shows that lower values of Pr_m will generate considerably lower black hole threading flux and this result is confirmed in the relativistic regime as well. The fundamental difference between BZ power for high and low Prandtl numbers is a shift in magnitude. While the spin dependence is unchanged, the power for $Pr_m = 2$ is lower by about one order of magnitude. One final point is in order. The outer boundary condition at $r = 54r_g$ is fixed which means that field dragging by the disk towards the black hole will generate bending of field lines that is greater than an analogous simulation in which the outer boundary is at a larger radial coordinate. Since the bending of field lines increases the diffusion term in equation 15, the choice of fixed outer boundary not only decreases the overall flux accumulation on the hole, it does so more for smaller choice of outer radial coordinate value. Like r_{dead} , r_{out} is an artificial aspect of our model whose physical value might be interpretable as some kind of load region where flux-freezing forbids flux lines from being dragged along with the field threading the accretion disk. In RGB, on the other hand, we did not fix the field at r_{out} , thereby allowing the field to be dragged unrestricted by the outer boundary value. Nevertheless, these caveats do not affect our basic qualitative result that the BZ luminosity is greater in the flux-trapping model and has the spin dependence shown.

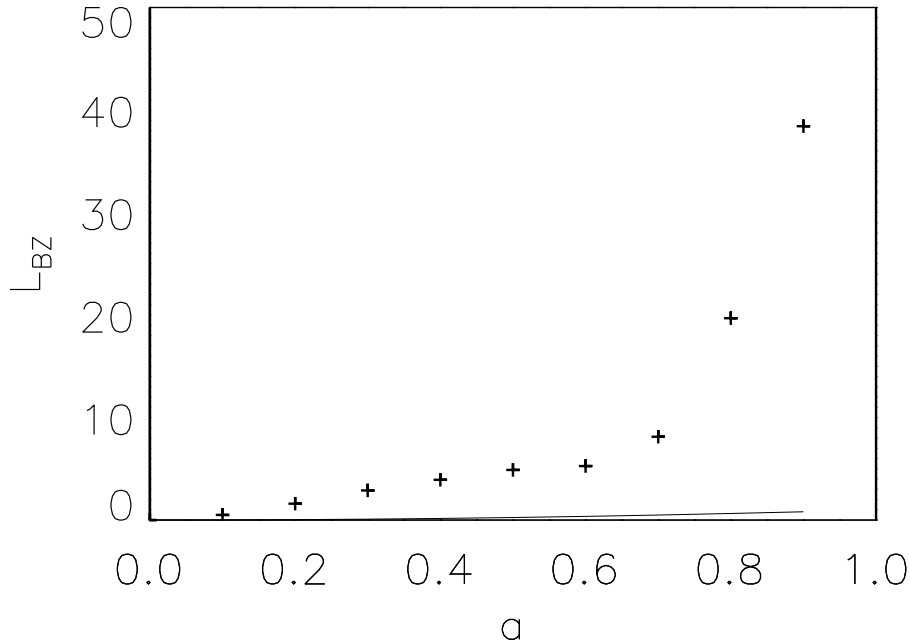


Fig. 8.—: The individual points label the Blandford-Znajek luminosity as a function of spin for $Pr_m = 20$. The solid line is the “classical” BZ power.

4. Discussion

In the previous section we showed that the magnetic field threading the black hole is always greater in the flux-trapping model which leads to larger BZ powers.

We will now show that our model has immediate application to the curious properties of jetted AGN in nearby elliptical galaxies.

Allen et al. (2006) used the *Chandra* X-ray observatory to study nine nearby X-ray luminous elliptical galaxies. Assuming central black hole masses given by the M - σ relation, *Chandra* measurements of the ISM temperature and density of scales $\approx 10pc$ from the cores of these galaxies could be used to deduce the rate at which ISM accretes into the gravitational potential of the black hole. These estimates are based on the simple spherical accretion picture of Bondi (1952). In addition, *Chandra* reveals ISM cavities that have been blown by jet activity from the central AGN. Using “PdV” arguments (and assuming that the cavities have an age given by their sound crossing time), the jet powers could be deduced. It was found that

$$P_{jet} \approx \eta \dot{M} c^2 \tag{22}$$

where $\eta \approx 3$. The object-to-object scatter about the correlation (eqn. 22) is small, with deviations in efficiency of only a factor of ≈ 2 .

Nemmen et al. (2006) have explored whether the Allen et al. correlation is a natural result of the BZ mechanism. Employing the Narayan & Yi (1995) advection dominated accretion flow (ADAF) model, which is likely appropriate for the low accretion rates found in these elliptical galaxies, Nemmen et al. estimated the strength of the magnetic field in the central disk as a function of accretion rate and then estimated the BZ efficiency, η_{BZ} , as a function of black hole spin, where

$$\eta_{BZ} \equiv \frac{L_{BZ}}{\dot{M}c^2}. \quad (23)$$

They showed that the Allen et al. results could only be reproduced if the elliptical galaxy black holes were all rapidly spinning and there was rather little mass loss in the accretion flow between the Bondi radius and the black hole. Although not as dramatic as in BZ, high spins are required for the hybrid model as well (Meier, 1999). Hence, all of the black holes in the Allen et al. sample would need to possess very close to the same, high prograde spin values; there is clearly a fine tuning problem with these models. For a review of the current state-of-the-art in measurements of black hole spin and why they should span a wide range, see Brenneman et al., 2009.

Assuming that the black holes in these elliptical galaxies are rotating in the prograde sense, the flux trapping model alleviates this fine tuning problem. We have taken the ADAF model of Nemmen and included the effects of flux trapping. The resulting η_{BZ} as a function of a for $a > 0$ is shown in Fig. 9 and compared with that of Nemmen et al. We caution the reader to ignore the solid line beyond $a = 0.9$ as it is simply a continuation of the fit that captures the behavior for lower spins. The absolute power that can be produced by the BZ mechanism in the flux trapping model is substantially higher (and slightly higher than that in the hybrid model); thus we can tolerate a much larger mass loss between the Bondi radius and the black hole. In addition, for intermediate values of prograde spin, the efficiency of the solid line representing the flux-trapping model is a flatter function of spin than the dashed line, producing a range of spin values compatible with the Allen et al. results. This η_{BZ} results from $Pr_m = 20$. For lower values of the Prandtl number down to $Pr_m = 2$, although the spin dependence of η_{BZ} is unchanged, the curve shifts downward. This forces the spin values of the black holes in the 9 AGN to be above about 0.6 as opposed to being above about 0.4 for $Pr_m = 20$. However, we remind the reader that in addition to the Prandtl number, the disk thickness and size also factor into the flux accumulation on the black hole. In fact, we could use $Pr_m = 2$ and increase the disk dead zone to 400 as opposed to 40 and get about the same magnitude of flux on the black hole. Alternatively, we could use $Pr_m = 2$, decrease the outer boundary to 200 and increase the disk thickness to 0.2 and again produce similar magnetic flux on the black hole. In fact, it would not be unreasonable to achieve greater magnetic flux values on the hole using $Pr_m = 2$ instead of $Pr_m = 20$ but increasing the other parameters in

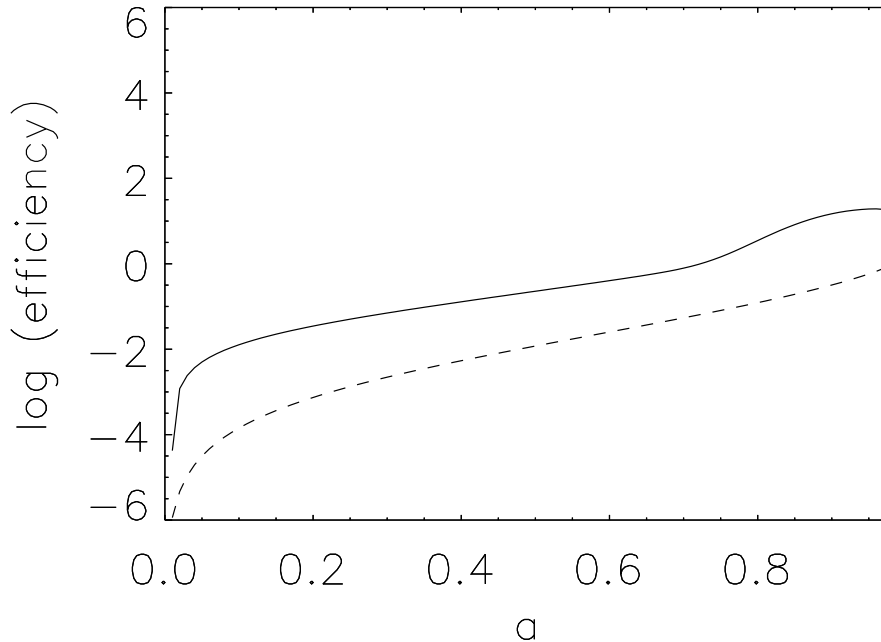


Fig. 9.—: The efficiency η_{BZ} vs. spin for the BZ model for a standard horizon-threading magnetic field (dashed line) vs. that in the flux-trapping model (solid line).

the disk. Ultimately, we suggest that this provides a more compelling exploration of the Allen et al. correlation than the more standard BZ model of Nemmen et al.

Finally, we note another interesting and novel prediction of the flux-trapping model. All other things being equal, accretion onto a rapidly rotating *retrograde* black hole will result in substantially higher BZ luminosities than possible in the prograde case (see Fig. 10). This is a direct consequence of the fact that the radius of marginal stability around a black hole that is rotating in a retrograde sense compared with the accretion disk will be *larger* than the corresponding Schwarzschild value, thereby leading to an even more dramatic “geometrical” enhancement of the magnetic flux trapped on the black hole. We suggest that some of the most powerful radio galaxies possess jets that are energized by accretion onto retrograde black holes. We note that recent *Suzaku* observations of the powerful broad-line radio galaxy 3C 120 found a broad iron emission line with a profile indicating an inner disk truncation at $r = 8.6_{-0.6}^{+1.0} r_g$ (Katooka et al. 2007), consistent with the location of the radius of marginal stability for a maximally rotating retrograde black hole ($r_{\text{ms}} = 9r_g$).

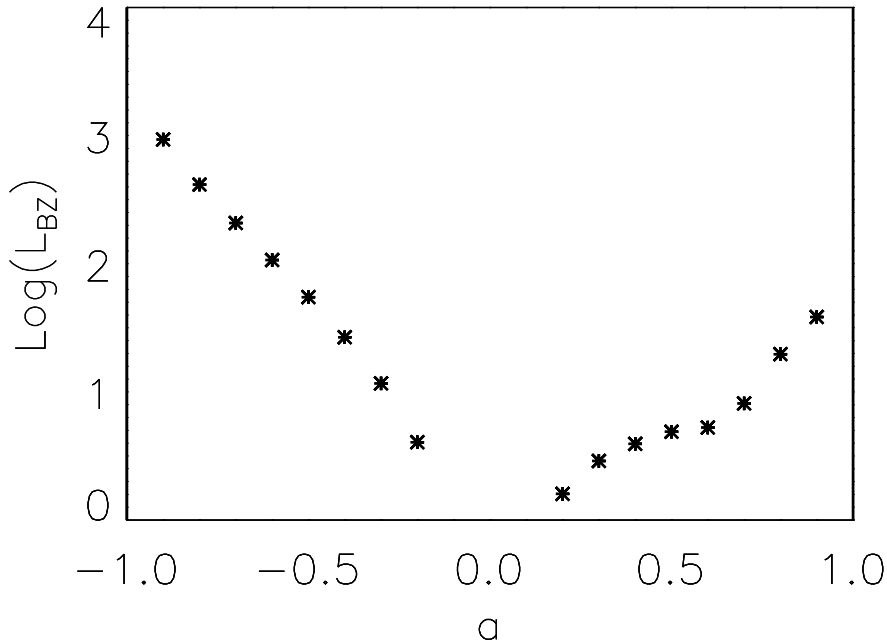


Fig. 10.—: Blandford-Znajek luminosity with $Pr_m = 20$ for the entire range of spins showing that for retrograde values the power can be more than one order of magnitude greater.

5. Comparison to recent GRMHD simulations

In this section we point out and comment on the fact that our results appear incompatible with recent GRMHD simulations. In McKinney & Gammie (2004), for example, the authors find that the powers for retrograde spins do not exceed the prograde ones and in GRMHD simulations, in general, the magnetic field on the black hole increases with larger prograde spin (e.g. De Villiers, 2005; Hawley & Krolik, 2006; McKinney, 2005) so there is no initial drop with lower prograde spins. The reasons for this difference appear to be twofold. GRMHD applies the flux-freezing condition (ideal GRMHD), which means that the magnetorotational instability (MRI) acts as a dynamo closer in to the black hole as the spin is more prograde since the inner edge of the disk is closer to the black hole. The validity of this result goes to the heart of the issue of physical vs. numerical resistivity and whether or not ideal GRMHD is less diffusive than realistic black hole flows. Within the context of ideal GRMHD, it is not surprising that retrograde BZ powers are not larger than prograde powers. The MRI operates further out for retrograde disks compared to the prograde ones and thus is incapable of increasing field strengths in the inner region. We should highlight a feature of retrograde powers in our model that may seem puzzling. In order to avoid

large discontinuities in the field line angular velocity in the transition region between the disk and the hole, we are forced to an angular velocity prescription that lowers BZ powers for all values of spin but in a way that increasingly lowers the power as the spin becomes more retrograde. This is because the discontinuity that would arise between the horizon and inner accretion disk is greater as the spin becomes more retrograde, so that avoiding a discontinuity has a greater effect on retrograde powers. But the plunge region boundary condition comes to the rescue, so to speak, in that it counteracts the otherwise large decrease in power that would result in large retrograde systems that stems from this smoothing out of the angular velocity profile in the transition region. The instantaneous advection assumption for the plunge region, in fact, produces sufficiently strong field on the black hole to compensate for the otherwise decrease in power. If we ignored the discontinuities and enforced an angular rotation of field lines on the horizon that is rigidly that of the black hole and one in the inner disk that is rigidly Keplerian, the powers for increasing retrograde spins would be even larger than shown. That solution, however, would not be self-consistent. In short, the plunge region boundary condition is fundamental in appreciating the difference between the flux-trapping model and ideal GRMHD. We should also point out that whereas our model is by assumption force-free everywhere outside the disk and plunge region plane, this condition exists only in specific regions in ideal GRMHD simulations. Specifically, the lack of a force-free configuration everywhere above and below the plunge region plane in GRMHD, means that the inertia of the gas is not negligible and therefore weighs in on the issue of magnetic flux accumulation on the black hole. Although the ability of the plunge region to enhance the field on the hole is weaker in GRMHD, it is nonetheless confirmed (for example, McKinney & Gammie, 2004). In RGB, it was shown that the enhancement of the hole-threading field with respect to the magnetic field in the inner disk depends not only on physical quantities such as disk Prandtl number but also on geometric aspects of the magnetized disk such as length and thickness. In addition, the enhancement on the hole compared to the inner disk depends also on the geometry of the initial magnetic field configuration (De Villiers et al, 2005; McKinney & Gammie, 2004). In other words, if the numerical solution in ideal GRMHD is less diffusive than the physical solution, and the initial conditions are such that the plunge region enhancement is small, then the magnetic field on the black hole can increase as the spin increases for all prograde values. In short, the issue of ideal vs. non-ideal GRMHD, as well as the issue of the initial conditions for the disk parameters and magnetic field, may conspire in ideal GRMHD to hide not only the effectiveness of the plunge region to enhance the B-field on the black hole compared to the inner accretion flow, but the spin dependence of this process as well. These issues cannot be addressed within the confines of our simple model and we limit our discussion, thus, to emphasizing that it may be more appropriate to compare our study to a future one that includes large scale magnetic fields treated within resistive GRMHD. In addition, one should keep in mind that this study is carried out in the thin disk approximation which is only assumed to occur for intermediate accretion rates. Furthermore, even for those intermediate accretion rates, it has recently been shown that thin-disk

accretion does not necessarily have to result (Fragile & Meier, 2009). Until radiative processes as well as physical resistivity are included, a realistic assessment of the detailed interaction between black holes and magnetized flows cannot be made. The effects discussed in this paper involve the spin dependence in a regime in which the dynamics of the plunge region is dominant, and in which the magnetized accretion flow does not act as a dynamo.

6. Conclusions

We postulated that given the dynamics of the plunge region of a thin black hole accretion disk, flux trapping can enhance the strength of the magnetic field threading the horizon by a significant factor. If the trapping behavior of the plunge region operates in as dominant a fashion as this study assumes, and if the energy emitted is BZ luminosity, one finds that the efficiency is a fairly flat function of spin for intermediate values of black hole spin. This allows one to follow the program of Nemmen et al to show that the enhancement due to the flux-trapping model on the BZ power is sufficient to explain the energies of the nine jets in the Allen et al sample including an attractive indeterminacy in the black hole spin. Finally, we suggest that some of the most powerful radio galaxies possess jets that are energized by accretion onto retrograde black holes.

Acknowledgments

The author thanks Christopher S. Reynolds as my graduate advisor for providing the opportunity to work on an interesting topic, for extensive discussion and for suggesting the application of the flux-trapping model to the Allen et al data. I also thank Ted Jacobson for helpful discussion on the relativistic equations, Cole Miller for useful suggestions on the draft as a whole, and David L. Meier for highlighting features of retrograde black hole accretion. Finally, I thank the anonymous referee for fundamental changes. D.G. is supported by the NASA Postdoctoral Program at NASA JPL administered by Oak Ridge Associated Universities through contract with NASA but also acknowledges partial support from NSF grant AST0205990.

References

- Allen, S.W., et al., 2006, MNRAS, 372, 21
Balbus, S. A., & Hawley, J.F., 1991, ApJ, 376, 214
Blandford, R. D., Payne, D.G., 1982, MNRAS, 199, 883

- Blandford, R. D., & Znajek, R. L. 1977, MNRAS, 179, 433
- Bondi, H., 1952, MNRAS, 112, 195
- Brenneman, L. Astro2010 Science White Paper
- Chandrasekhar, 1961, Hydrodynamic and Hydromagnetic Stability, Oxford University Press.
- De Villiers, J.P., Hawley, J.F., & Krolik, J.H., 2003, ApJ, 599, 1238
- De Villiers, J.P., Hawley, J.F., Krolik, J.H., Hirose, S., 2005, ApJ, 620, 878
- Fragile, P.C., Meier, D.L. 2009, ApJ, 693, 771
- Ghosh, P., Abramowicz M.A., 1997, MNRAS, 292, 887
- Hirose, S., Krolik, J.H., De Villiers, J.P. & Hawley, J.F., 2004, ApJ, 606, 1083
- Komissarov, S.S., 2001, MNRAS, 326, 41
- Livio M., Ogilvie G.I., Pringle J.E., 1999, ApJ, 512, 100
- Lubow, S.H., et al., 1994, MNRAS, 268, 1010
- Macdonald, D.A., 1984, MNRAS, 211, 313
- McKernan, B., et al., 2007, MNRAS, 379, 1359
- McKinney, J.C., Gammie C.F., 2004, ApJ, 611, 977
- McKinney, J.C., 2006, MNRAS, 368, 1561
- Meier, D.L., 1999, ApJ, 522, 753
- Meier, D.L., 2001, ApJ, 548, L9
- Moderski R., Sikora M., Lasota J.-P., 1998, MNRAS, 301, 142
- Narayan, R., Yi, I., ApJ, 1995, 452, 710
- Nemmen R.S., et al., 2007, ApJ, 377, 1652
- Reynolds, C.S., et al, 1996, MNRAS, 283, 873
- Reynolds, C.S., & Begelman, M.C., 1997, ApJ, 487, 135
- Reynolds, C. S., Garofalo, D., & Begelman, M. 2006, ApJ, 651, 1023
- Thorne, K. S., Price, R. H., & Macdonald, D. A. 1986, Black Holes: The Membrane Paradigm (New Haven: Yale Univ. Press)

Wardle, J.F.C, et al, 1998, *Nature*, 395, 457

Znajek, R.L., 1978, *MNRAS*, 185, 833

Velikhov, F., 1959, *Soviet Phys-JETP*, 36, 1398